Advances in Locally Varying Anisotropy With MDS

J.B. Boisvert and C. V. Deutsch

Often, geology displays non-linear features such as veins, channels or folds/faults and results in complex spatial relationships. The complex relationships manifest themselves as nonstationary features to be incorporated into numerical modeling. The overall methodology suggested in this paper for incorporating locally varying anisotropy (LVA) is to consider how two locations in space are related. Normally, the straight line path is used to relate locations; however, when nonlinear features exist, the appropriate path between locations follows the features, such as along a channel in a fluvial deposit. The distance between points is calculated along this non-linear path and converted to a covariance using a standard variogram. Because the non-linear path is a non-Euclidian distance metric, positive definiteness of the resulting kriging system of equations is not guaranteed. Multidimensional scaling (MDS) is used to ensure positive defiantness while the Dijkstra algorithm is used to determine the path between locations. A number of papers have been presented in past CCG reports that have discussed LVA. The intention of this paper is to present a consistent methodology that can be used to incorporate LVA into geostatistical modeling. Small synthetic examples are presented for illustrative purposes while paper 203 in this report presents a more detailed case study incorporating LVA into a larger example.

Introduction

In a geological setting, anisotropy refers to how continuous a deposit is in different directions. Often, deposits display the type of anisotropy shown in Figure 1. Anisotropy within geological formations can be exploited to increase the accuracy of modeling. If the direction and magnitude of anisotropy are well understood, they can be transferred into modeling to improve performance. Consider an LVA field modeled after the hand drawn directions on Figure 1 and two drill holes through the deposit. Techniques, such as inverse distance, that do not normally consider anisotropy, cannot capture the horizontal continuity of the deposit (Figure 2 left). Other techniques, such as kriging, provide disappointing results because only a single direction of continuity can be incorporated into the modeling (Figure 2 middle). More geologically realistic results can be obtained by considering that the anisotropy varies locally (Figure 2 right); however, incorporating LVA in even this simple case is difficult. More complex anisotropy fields, such as Figure 1 left, are challenging.

The geological cross sections in Figure 1 provide the motivation for considering LVA; traditional geostatistical modeling would only consider a single direction of anisotropy. Estimates of resource volume in these situations would be greatly improved by considering LVA. This paper integrates LVA into geostatistical modeling.

Figure 1: Cross sections displaying LVA. Left: Folding and faulting caused by the San Andreas Fault (www. strike-slip.geol.ucsb.edu). Right: Folding in the northern Rocky Mountains (www. mkutis.iweb.bsu.edu).

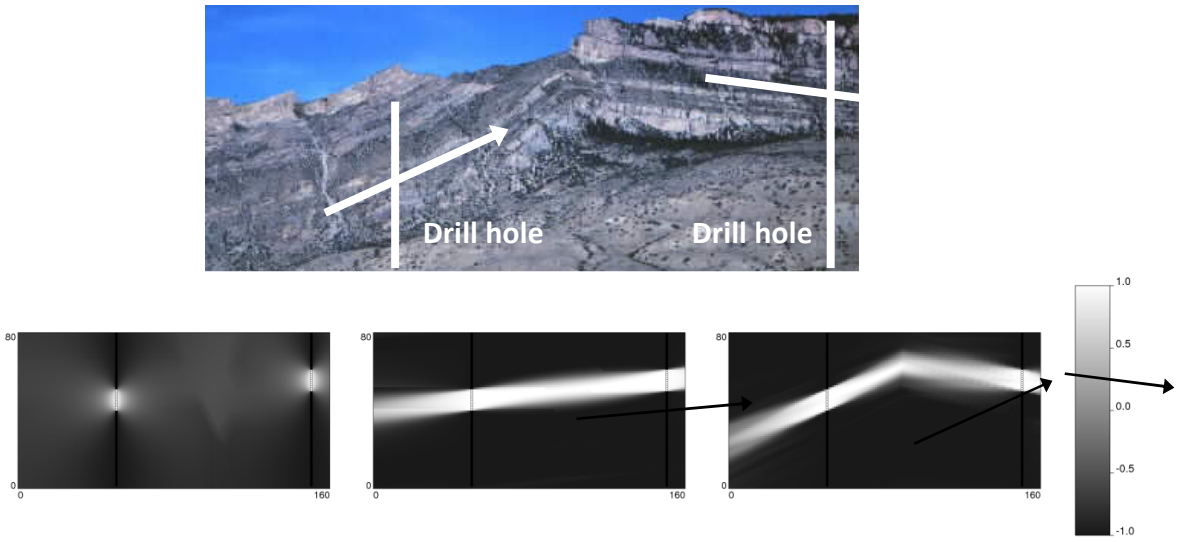

Figure 2: Top: cross section with the two drill holes (www.mkutis.iweb.bsu.edu). Lower Left: inverse distance estimation. Lower Middle: Traditional kriging. Lower Right: Kriging considering LVA.

Methodology

At the core of resource estimation with geostatistics is spatial prediction of variables from sparse sample data. From these spatial predications of grade, porosity, saturation and concentration, resource and reserve calculations can be made. LVA is incorporated into the spatial predictions of variables by using the optimized shortest path distance (SPD) between locations. The SPD is utilized in a modified version of inverse distance weighted interpolation (IDW) to introduce the idea of spatial predictions with nonlinear paths as well as to demonstrate the effects of using the SPD in geostatistical modeling.

Kriging and sequential Gaussian simulation (SGS) are geostatistical tools often applied in resource evaluation studies as an alternative to IDW. They require the solution to a positive definite system of equations. MDS techniques are introduced to guarantee the positive definiteness of this system of equations.

Methodology: Inverse Distance

The most common form of spatial interpolation is the prediction of estimates from a weighted average of nearby data (Babak and Deutsch 2008). The concept is to determine weights, λ_α, (Equation 1) to assign to surrounding data, z_α, and generate an estimate, z^*, at an unsampled location, $\mathbf{u}$. With IDW, the weights are obtained by applying an inverse power, ω, to the distance between the unsampled location and the nearby samples (Equation 2).

$$z^*(\mathbf{u}) = \sum_{\alpha=1}^{n} \lambda_\alpha \, z_{\alpha(u_\alpha)} \qquad \mathbf{1}$$

where n is the number of data available for estimation.

$$\lambda_\alpha = \frac{\frac{1}{d_\alpha^\omega}}{\sum_{\alpha=1}^{n} \frac{1}{d_\alpha^\omega}} \qquad \mathbf{2}$$

The incorporation of the SPD into IDW is straightforward, the distance is replaced with the SPD:

$$\lambda_\alpha = \frac{\frac{1}{SPD_\alpha^\omega}}{\sum_{\alpha=1}^{n} \frac{1}{SPD_\alpha^\omega}} \qquad \mathbf{3}$$

Paper 110 in CCG report 10 presents a detailed description of the methodology for the calculation of the SPD in the presence of LVA. In summary, the methodology used to calculate the SPD implements the Dijkstra algorithm (Dijkstra 1959) to determine the shortest path in a graph where the graph is constructed by considering the grid cell blocks as nodes connected by edges. The distance along an edge (Figure 3) is the anisotropic distance calculated using the local anisotropy specification.

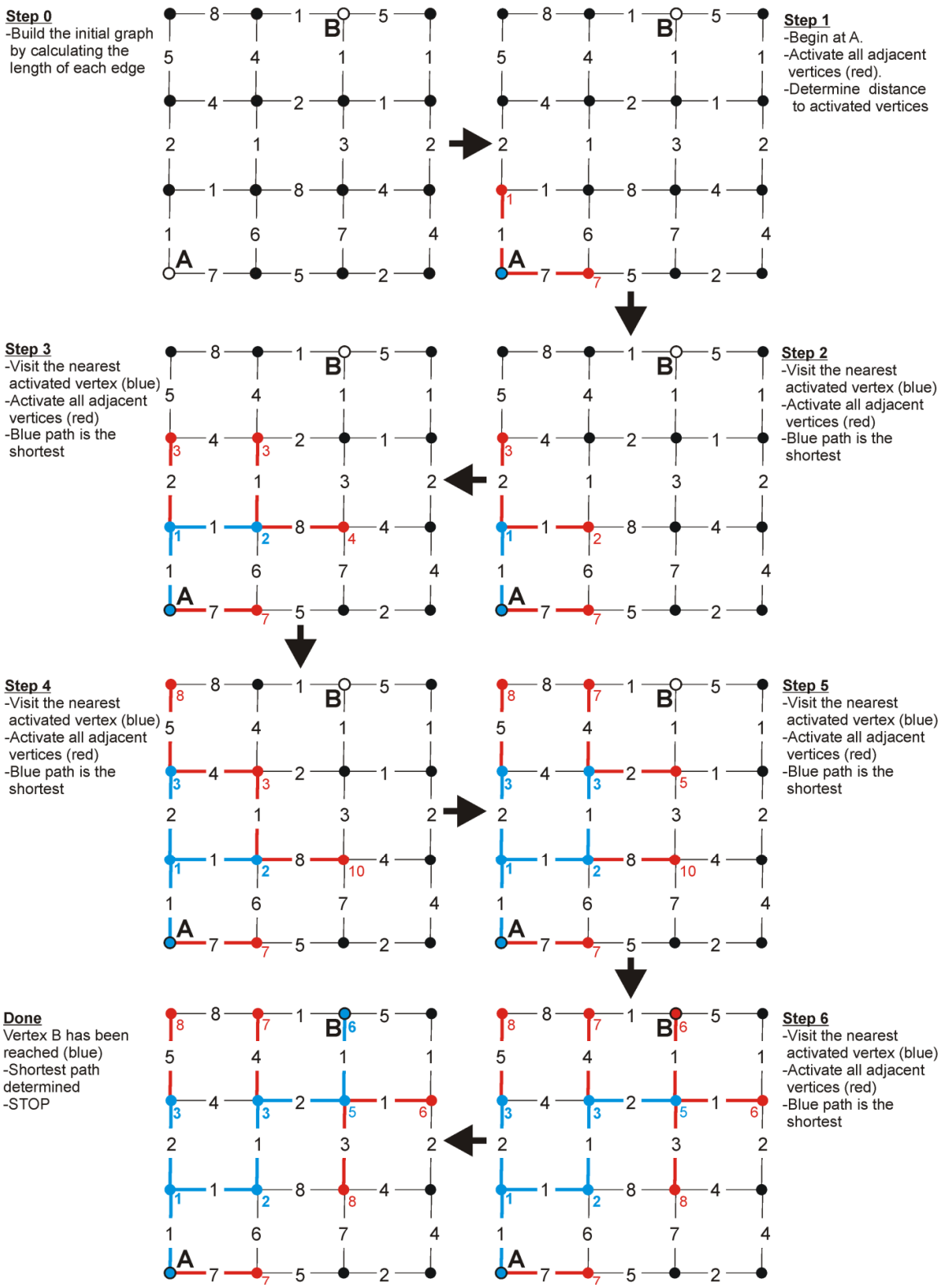

Figure 3: Dijkstra algorithm steps. Grid cell centers are considered nodes (circles).

Using the weights in Equation 3 the IDW estimate maps are constructed. Consider an anticline LVA field with three drillholes (Figure 5). There are a total of 78 sample data, thus the distance matrix (**D**) between the 2601 grid nodes and the 78 sample data (Figure 4) is required to calculate the necessary weights. Each distance is calculated using the Dijkstra algorithm. The resulting estimated map is shown in Figure 5.

The locally varying dips of the anticline are well reproduced in Figure 5. Often IDW is used as an exploratory technique in the early stages of a geostatistical project; however, there are situations when it is preferred, such as when the variogram is difficult to infer for a particular data set. Notwithstanding the simplicity of IDW with LVA, if an estimated map is required it is more common to apply kriging because estimates are optimal in the least squared error sense.

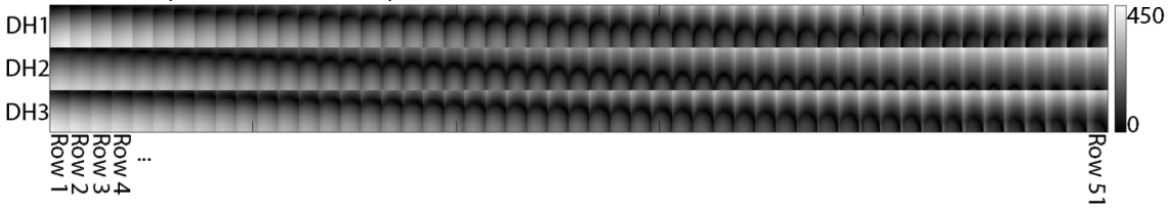

Figure 4: Distance matrix (**D**) between 78 data (3 drill holes with 26 data per drill hole). Each row of the distance matrix represents the distance from one of the 78 samples to the 2601 cells in the model.

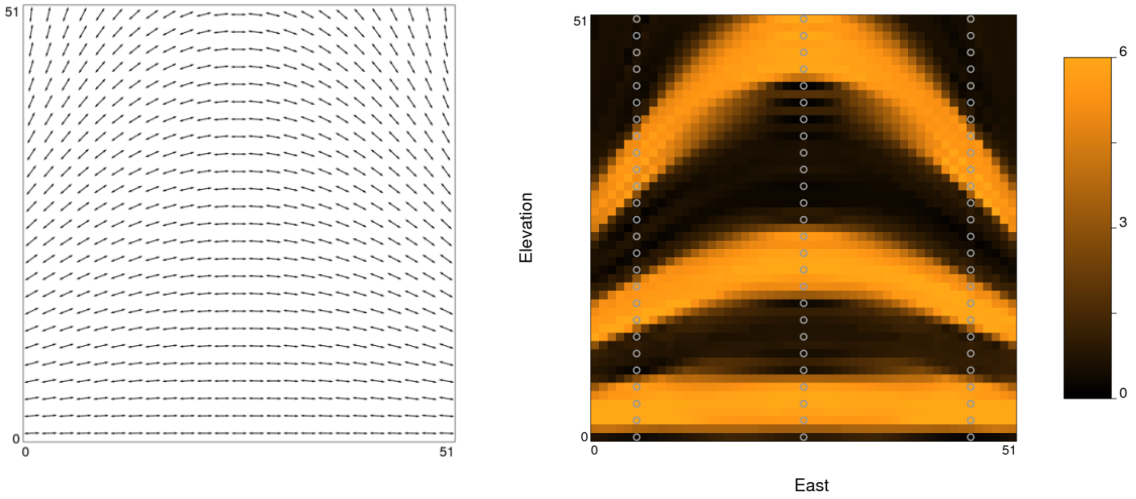

Figure 5: Left: Anticline LVA field with a constant anisotropy of 10:1. Right: Spatial estimates using IDW.

Methodology: Kriging

Incorporating the SPD into kriging and SGS is not as straightforward as with IDW. The mathematical foundation of kriging and SGS is based on the solution of a positive definite system of equations derived from the well known kriging equations (Equation 4).

$$\sum_{\beta=1}^{n} \lambda_\beta C(\mathbf{u_\alpha}, \mathbf{u_\beta}) = C(\mathbf{u}_?, \mathbf{u_\alpha}) \quad \alpha = 1, \dots, n \qquad \textbf{4}$$

If the covariances in Equation 4 form a positive definite covariance matrix, the solution to the kriging system of equations is unique and can be determined (Christakos, 1984 and Cressie, 1991). Normally, positive definiteness is ensured by using an Euclidean distance metric and a covariance function that has been shown to result in a positive definite covariance matrix (Christakos 1984); however, covariance functions that guarantee positive definiteness when used with the SPD metric have yet to be developed nor has it been shown that such covariance functions even exist. As an alternative to developing covariance functions that ensure positive definiteness with SPD, the SPD metric is mapped to a high dimensional Euclidean space using MDS algorithms. In the high dimensional Euclidean space, valid covariance models can be used to ensure positive definiteness; however, some accuracy is lost and the distance reproduction in the higher dimensional space is not exact (paper 111 in CCG report 10).

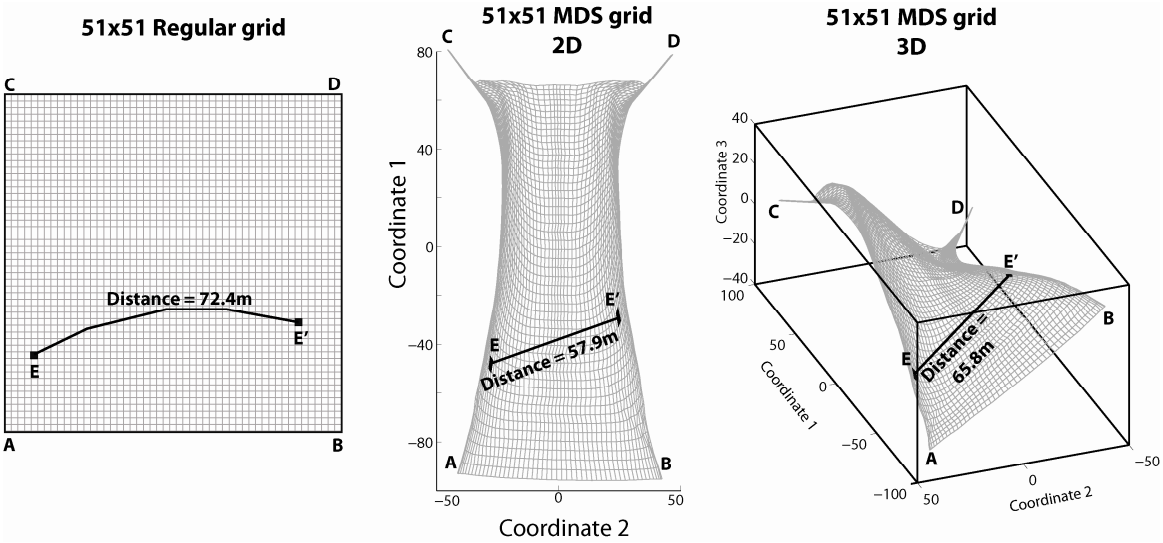

Figure 6: Transformation of a 51x51 anticline LVA field. The length of the path E-E' is shown in all coordinate systems. Note that in the transformed coordinate system (middle and right) there are 2600 dimensions (2601– 1) but visualization is only possible in the first 2 or 3 dimensions.

A covariance function (i.e. variogram, correlogram, etc) is required to calculate the covariance between locations separated by a lag vector (**h**). Once the covariance function is known the kriging weights are solved for all unsampled locations in the geostatistical model and a smooth estimated map is generated. Kriging is implemented by the following algorithm:

Step 1: Generate the LVA field (paper 103 in CCG report 11).

Step 2: Calculate the distance matrix between points with the Dijkstra algorithm (paper 110 in Report 10).

Step 3: Perform MDS to embed all cells in a high dimensional Euclidean space (paper 111 in Report 10).

Step 4: Model an isotropic variogram to obtain the covariance between locations given the SPD.

Step 5: For every grid cell:

a. Determine the nearest *n* neighbors
b. Calculate the required *n* by *n* distance matrix
c. From the *n* by *n* distance matrix, calculate the covariance matrix using the modeled variogram
d. Solve the resulting system of equations to determine weights for each datum
e. Calculate the kriging mean and error variance

Kriging for a small example is shown in Figure 7. Step 3 is necessary to ensure that a unique solution to the kriging equations exists (Curriero 2005). The following section discusses steps 4 and 5. Detailed discussion on steps 1 through 3 can be found in the aforementioned CCG reports. Kriging requires the following inputs:

1. The LVA field (paper 103 in CCG report 11).
2. The value of *n*. In practice this value is usually set between 20-50 depending on the application.
3. The isotropic variogram. This variogram is modeled from the available sample data.
4. The necessary parameters for MDS (paper 111 in CCG report 10)

Searching for nearby data

Kriging can be applied using all available data to estimate at an unsampled location. Each datum receives a weight from solving the kriging equations (Equation 4); this is global kriging. Global kriging is preferred in situations where there are few data and the modeling area is stationary; however, when many samples are available, it is often impractical due to CPU requirements. It is common to restrict the number of data used to estimate a given location to the nearest *n* data in the local neighborhood (Deutsch 1998). This step in kriging requires searching for the *n* nearest neighbors of the estimation location. One search that has been implemented effectively is the super block search (Deutsch 1998). In the proposed methodology the available data are embedded in a *q*-dimensional space, use of the super block search

strategy would require indexing n^q super blocks, which is prohibitive in terms of memory requirements. An alternative search strategy is to use a *k*-dimensional tree (*k*d tree). The *k*d tree is a binary search tree specifically designed for searching in high dimensional space (Kennel 2004).

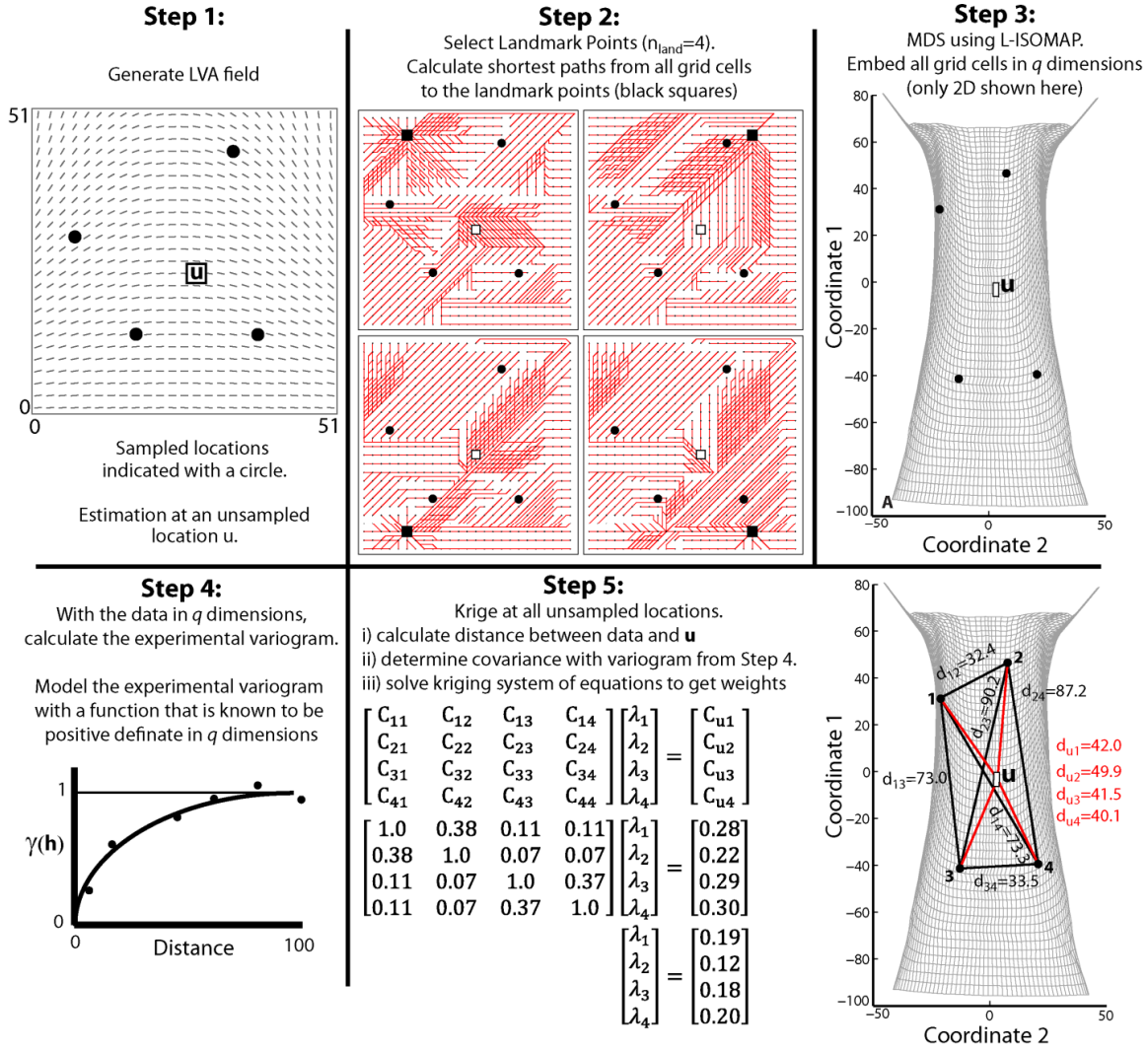

Figure 7: Kriging with LVA explained.

An Isotropic Covariance Function

Kriging requires a function to calculate the covariance between locations, such as the variogram, γ(**h**). The variogram represents the variance between two locations in space separated by a lag vector, **h** (Equation 5). The variogram is often modeled by first calculating experimental variogram points from the method of moments technique (Equation 6) and fitting them with an analytical function (Figure 8).

$$\gamma(\mathbf{h}) = C(0) - C(\mathbf{h}) \quad (5)$$

$$\gamma(\mathbf{h}) = \frac{1}{N(\mathbf{h})}\sum_{i=1}^{N(\mathbf{h})}(x_i - y_i)^2 \quad (6)$$

The experimental variogram can be calculated for discrete values of **h** by pairing sampled data values separated by an appropriate lag, **h**, and calculating the variance. The covariance can depend on the direction of **h** as well as the magnitude; however, an isotropic covariance function that is independent of direction is applied in LVA kriging. The magnitude of **h** separating two locations in space, say points *a* and point *b*, can be determined by calculating the Euclidean distance between locations once they have been embedded in *q* dimensions (Equation 7).

$$d_{a-b}^2 = \sum_{i=1}^{q} \left(l_a^i - l_b^i\right)^2 \quad (7)$$

where l_a^i is the coordinate of point a in the i^{th} dimension.

Consider the Walker Lake data set (Isaaks and Srivastava, 1989). The experimental variogram can be generated after applying MDS. The experimental variogram is calculated for the first 3 dimensions (Figure 8 below right) and displays very little anisotropy, all three directions are virtually identical with respect to the variogram. Of concern is the reduction in the range of the variogram, initially the range of correlation is between 20m-50m while after applying MDS the range is reduced to ~10m. This is because of the imperfect embedding in the new space. This can be improved upon if more dimensions are considered with MDS (Figure 8 below right).

The adoption of an isotropic covariance function is justified as the embedding of the grid removes all anisotropy from the data (Sampson and Guttorp, 1992), this is the effect seen in Figure 8 (below right) where the variogram is nearly identical in the first three embedded dimensions. An isotropic variogram in q dimensions can reproduce LVA because these features are captured by the inter-point distance matrix generated from the Dijkstra algorithm, rather than in an anisotropic variogram. Considering anisotropy in the higher dimensional space would be redundant as the anisotropy should be captured in the underlying LVA field used to determine the shortest path between locations. Moreover, if anisotropy is considered in the q-dimensional space it would be difficult to predict the parameters necessary to define the analytical covariance function. It has been the authors experience that often q>100. Generating an anisotropic variogram that considers each of these 100+ dimensions would require sufficient data density to inform each dimension.

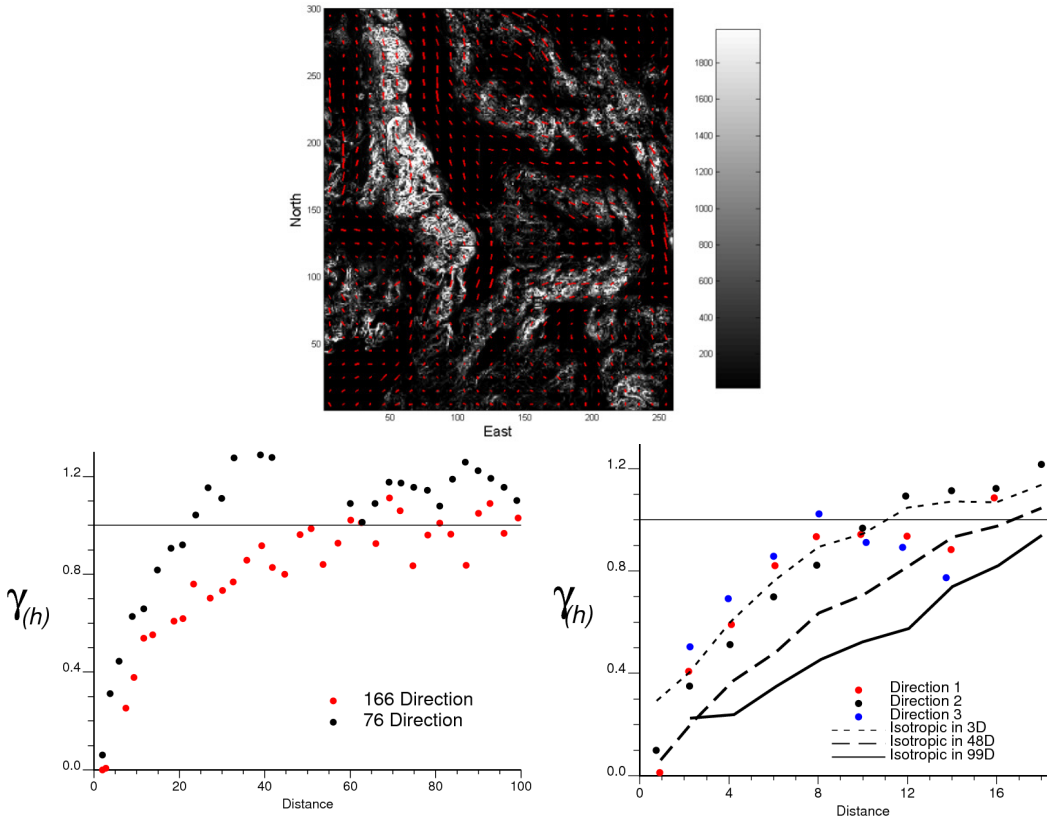

Figure 8: Above: Lines indicate the direction of continuity, the magnitude is proportional to the length of the line. Below Left: Traditional experimental variogram. Below Right: Experimental variogram considering data embedded with MDS.

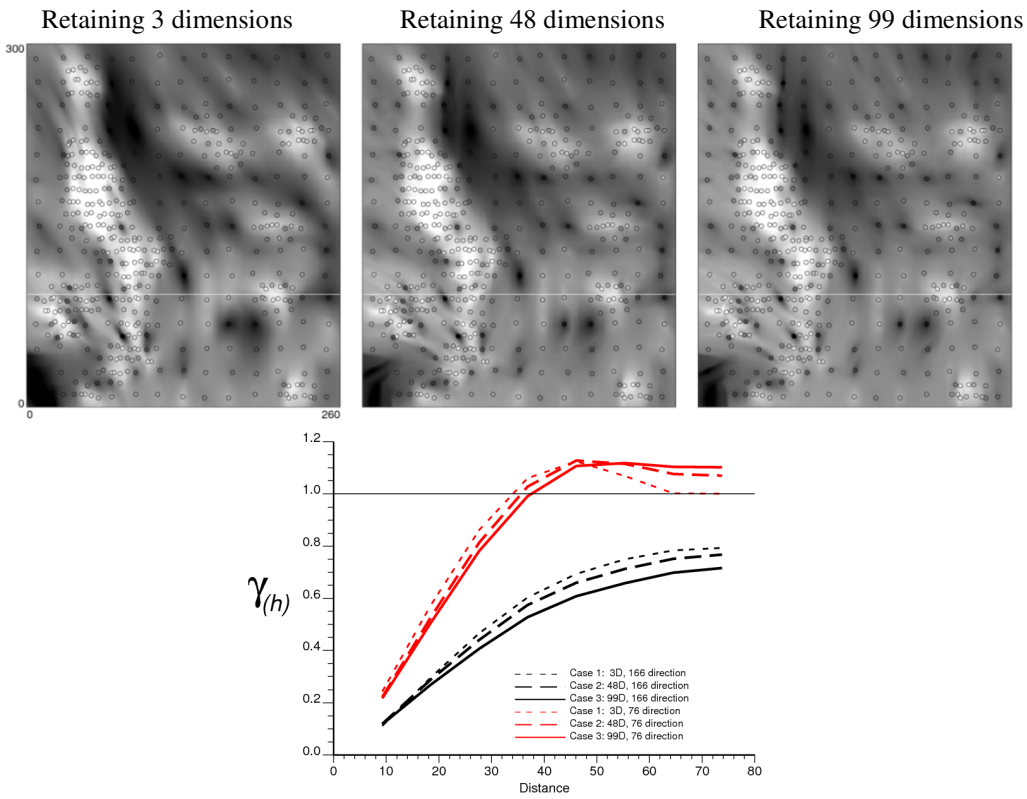

Figure 9: Above: Kriging, color scale is from 0 (black) to 1700 (white). Below: Variograms for each case. Note the variance of the kriged estimates is less than the variance of the data.

Kriging requires the variogram using the SPD so that covariance can be determined. The experimental variogram is calculated from Equation 6; an example experimental variogram is shown for the Walker Lake data (Figure 8). A positive definite function must be fit to the available experimental variogram because the experimental variogram does not produce kriging system of equations that are positive definite. Table 1 lists the common variogram models used in geostatistics.

Not all functions in Table 1 are positive definite for all dimensions. Extensive literature exists that deals with the mathematical validity of covariance functions as well as testing potential functions for positive definiteness (Christakos 1984, Matheron 1973, Curriero 2005). Because the available sample data are located in a q dimensional Euclidean space, the selected variogram function must be positive definite in q dimensions (Curriero 2005). If q is selected to be 3, then all variograms commonly used in practice are permissible. However, to increase accuracy it is recommended that q be as large as possible, thus limiting the available variogram models.

Table 1: Some known positive definite variance functions.

Functions Name	Equation	dimensions for positive definiteness	Comments	Relevant References
Spherical	$\gamma(\mathbf{h}) = 1.5\frac{h}{a} - 0.5\left(\frac{h}{a}\right)^3$	(see comment)	Could be made positive definite in any dimension: consider volume of intersecting hyper spheres	Deutsch 1998
Exponential	$\gamma(\mathbf{h}) = 1 - exp\left(-\frac{(3h)^\omega}{a^\omega}\right)$ $0 < \omega < 2$	Any Dimension	Positive definite in any dimension.	Deutsch 1998
Matern Class	$\tau^2 + \sigma^2\left\{\left(2^{\kappa-1}\Gamma(\kappa)\right)^{-1}\left(\frac{\|\mathbf{h}\|_\alpha^{\beta/2}}{\phi}\right)^\kappa K_\kappa\left(\frac{\|\mathbf{h}\|_\alpha^{\beta/2}}{\phi}\right)\right.$	Any Dimension	See references for more details.	Curriero 2005

The Kriging Variance

An interesting result of considering LVA is that the kriging variance is bounded by traditional kriging with a single anisotropy specification. Consider a simple channel example where the anisotropy is 10:1 inside the channel and 1:1 outside the channel. The range of the variogram used in LVA kriging is 8 units with an exponential function (Table 1). The resulting kriging variance is bounded by simple kriging with an omni-directional range of 8units and simple kriging with an omni-directional range of 80units (Figure 10). Simple kriging with an omni-directional range of 80units represents a best case, minimum variance scenario for LVA kriging; the shortest path distance cannot be smaller than considering the straightline path between points with a range equivalent to 80units. Similarly, simple kriging with an omni-directional range of 8units represents a worst case, maximum variance scenario for LVA kriging; the SPD is smaller than or equal to the straightline path between points with a range equivalent to 8units. As such, the variance for LVA kriging (considering a monotonically decreasing covariance function) lies between the two extremes.

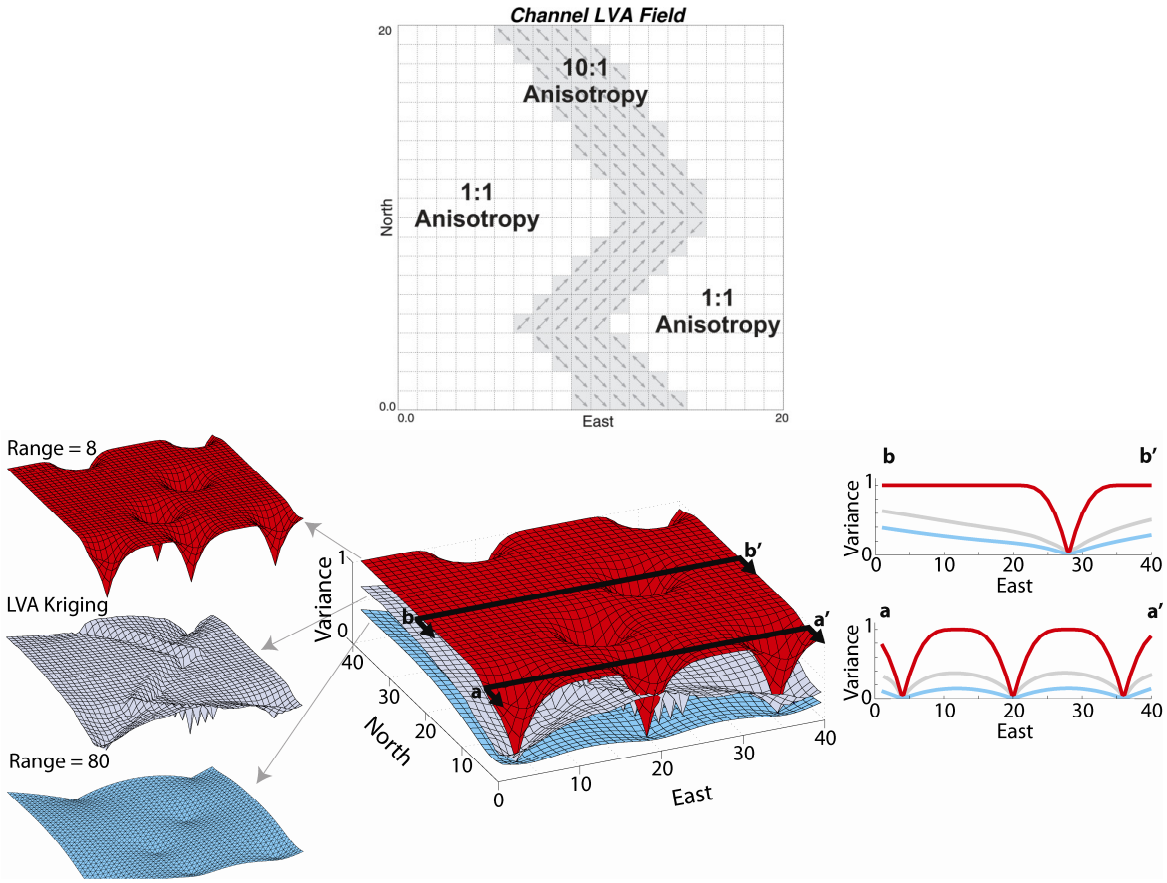

Figure 10: Above: LVA field. Below: Variance with simple kriging (range = 8units and range = 80units) and variance with LVA kriging. Section aa' and bb' are shown to the right.

Methodology: SGS

The motivation for considering SGS is the reproduction of the correct variability seen in the original data. This is accomplished by generating a number of different equi-probable realizations of the desired random function Z(**u**). SGS is similar to kriging; first, a location, **u**, is selected and kriging is performed using the nearby data to determine the parameters of the local Gaussian distribution, $N(m_u,\sigma_u)$. A random value is then drawn from the $N(m_u,\sigma_u)$ distribution which constitutes a simulated value at **u**. This simulated value is added to the growing list of simulated nodes and is used when simulating all successive locations. SGS is described in detail in Figure 11.

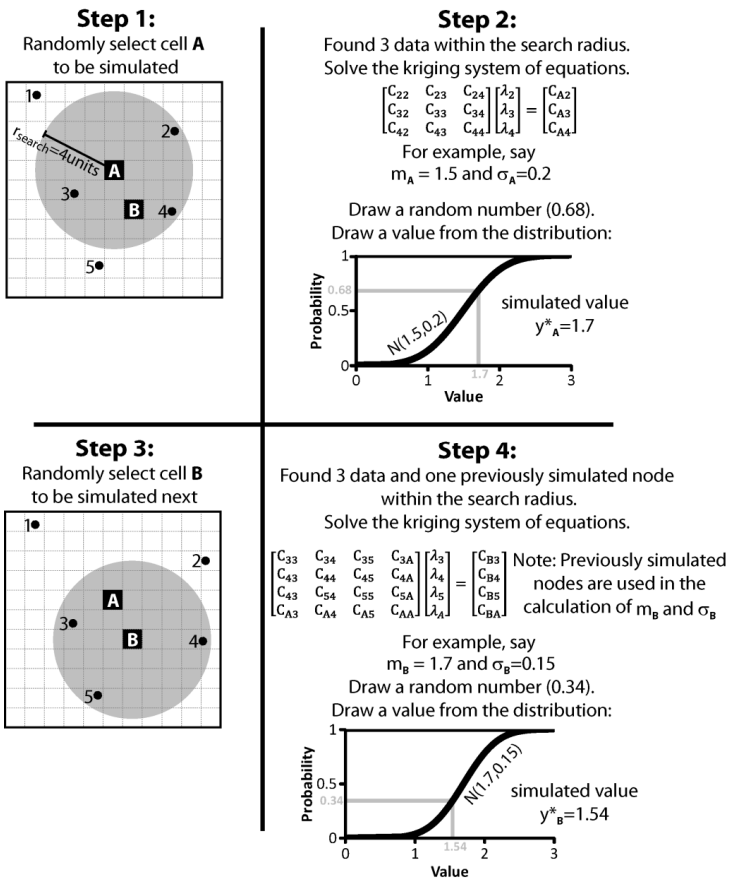

Figure 11: SGS explained. Simulation of node A is followed by node B. This process is sequentially repeated for all locations. Previously simulated nodes are included when simulating successive nodes.

The necessary inputs to SGS are identical to those discussed in kriging: an LVA field; the number of nearby data to consider; an isotropic variogram; and the necessary parameters for MDS. There are two aspects of SGS that significantly increase computational requirements and require practical solutions. The first aspect is the use of previously simulated locations when performing SGS. As the sequential process proceeds, more simulated nodes become available. When simulating at **u**, the growing list of previously simulated nodes must be searched to find the nodes in the neighborhood of **u**, which is more computationally demanding than simply searching for nearby sample data as with kriging. The second aspect of SGS that increases computational requirements is the common practice of generating multiple (100+) realizations. While the CPU time required to generate a single realization is reasonable the time required to generate 100 realizations would not be practical. This section presents solutions to these two issues.

Searching for nearby previously simulated nodes

Implementation of the SGS algorithm often requires the user to limit the number of data used to improve CPU performance. Not all data can be considered as the solution to the kriging system of equations would require excessive CPU time; therefore, it is common to use *m* nearest data to the simulation location and ignore all other data (Deutsch 1998). All available conditioning data, such as drillholes or wells, are assigned to grid nodes. This is required for the usage of the Dijkstra algorithm when determining the SPD between locations. As such, no distinction is made between previously simulated nodes and the initial conditioning sample data; data behave as previously simulated nodes that are fixed for each realization. The problem then reduces to finding the *m* nearest informed nodes to a given

location, **u,** in a model with *N* total nodes. This can be accomplished with a *k*d tree. All *N* grid locations are loaded into the search tree and the nearest informed nodes are returned (Kennel 2004).

Considering multiple realizations

The CPU requirements of SGS in this implementation are significantly larger than considering constant anisotropy because of the calculation of covariance between locations. When anisotropy is constant, a covariance lookup table can be created to determine the covariance between grid cells given their xyz indices (Deutsch, 1998). This is not possible with LVA for two reasons (1) the data are no longer on a regular grid after MDS and (2) the data are in *q* dimensions and would require a *q* dimensional lookup table that would be too large to store in RAM. Regardless of the memory requirements, a covariance lookup table is only possible with regularly gridded data. Thus, when simulating, the distances between all informed nodes within the local neighborhood must be calculated as in Equation 7.

Multiple realizations, each with a different random path, are typically considered in a geostatistical work flow (Deutsch, 2002). Generating realizations with the same random path produces kriging matrices that are identical for all realizations. The kriging matrices can be stored and used for all realizations to improve CPU time by a factor of *r*, where *r* is the number of realizations considered. The calculation of the necessary distances between locations (Equation 7) cannot be avoided but if the same random path is used for all realizations, these distance calculations are identical for all realizations.

A different random path is used for each realization because some practitioners believe artifacts may arise otherwise. Artifacts do occur if an axis aligned sequential path is selected (Isaaks 1991); however, there is no evidence that generating realizations using the same *random* path produces artifacts. The concern is that considering only a single random path may produce realizations that are *too similar,* that is, realizations that to do not properly span the space of uncertainty in the random variable modeled, Z(**u**). This can be assessed by comparing the statistics of realizations produced with the same random path to the statistics of realizations produced with different random paths. Consider the Walker Lake data set, the same data set used in Isaaks (1991) to show that an axis aligned path produces artifacts. 50 realizations are generated with a single random path and compared to 50 realizations generated with different random paths, no visual artifacts are noted (Figure 12). Two statistics are assessed (1) the histogram of the realizations and (2) the variogram of the realizations. If use of a single random path does not adequately span the space of uncertainty, the variations in these measured statistics would be reduced. Figure 13 indicates that there is no reduction in the space of uncertainty for either the histogram or variogram when using a single random path for each realization; however, this result cannot be generalized to all models. *Unlucky* paths that generate realizations with artifacts remain possible. Realizations with different random paths could be generated but the necessary CPU time is impracticable for any reasonably sized geomodel.

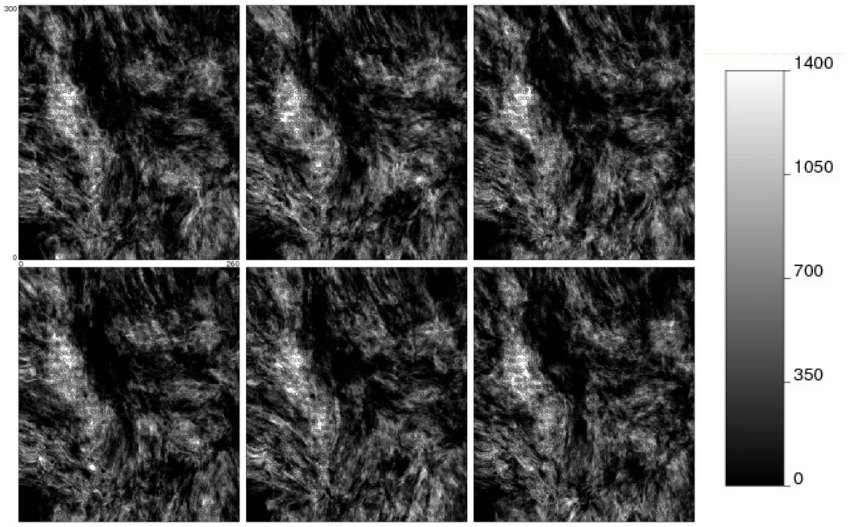

Figure 12: Above: Three realizations using different random paths. Below: three realizations using the same random path.

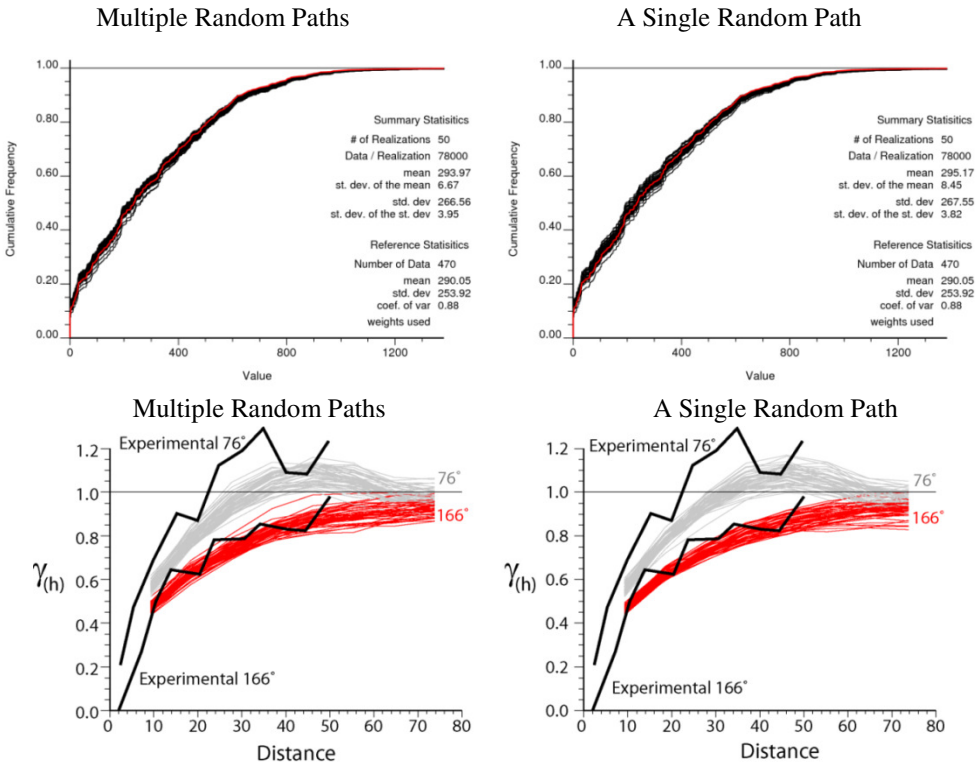

Figure 13: Above: Histograms of 50 realizations. Below: Standardized variograms of 50 realizations. SGS with LVA does not explicitly reproduce the experimental variograms in the 76˚ and 166˚ directions as these directions are not used in the modeling process. Of interest here is only the variability of the resulting variograms using a single random path.

Methodology: Summary

The methodology for implementing SPD with inverse distance, kriging and SGS is summarized below:

Inverse distance:

Step 1: Calculate the SPD with the Dijkstra algorithm

Step 2: Determine the weights to assign to conditioning data with the typical inverse distance methodology (Equation 3)

Kriging:

Step 1: Generate the LVA field.

Step 2: Calculate the initial distance matrix between the required points with the Dijkstra algorithm.

Step 3: Perform MDS to embed all cells in a high dimensional Euclidean space.

Step 4: Model an isotropic variogram. This variogram is used to obtain the covariance between locations given the SPD.

Step 5: For every grid cell, determine the nearest *n* neighbors and solve the resulting system of equations to determine the kriging weights for each datum.

SGS:

Step 1: Generate the LVA field.

Step 2: Calculate the initial distance matrix between the required points with the Dijkstra algorithm.

Step 3: Perform MDS to embed all cells in a high dimensional Euclidean space.

Step 4: Model an isotropic variogram. This variogram is used to obtain the covariance between locations given the SPD.

Step 5: Visit every grid cell in a random order and determine the nearest *n* neighbors. Solve the resulting system of equations to determine the kriging weights for each datum.

Step 6: Draw a simulated value at the estimation location for each realization (the same random path is used for all realizations).

Synthetic Example

The goal of this paper is to generate geostatistical models that display nonstationary anisotropy. A single specification of anisotropy is often insufficient to fully describe natural phenomenon. Figure 14 contains a number of synthetic examples that highlight some of the types of geological features that can be reproduced with LVA including (1) folding (2) non linear channel/vein deposits (3) smoothly changing local directions of anisotropy.

Conclusions

IDW techniques have the advantage of simplicity. Moreover, the positive definite limitation of kriging and SGS does not apply to IDW because a system of equations is not solved, the weights are calculated directly from the SPD. This also implies that MDS algorithms are not required to perform IDW. The only computational requirement is the calculation of the necessary distances with the Dijkstra algorithm.

Ideally, when implementing kriging and SGS a covariance function that ensures positive definiteness with the SPD metric would be available; however, no such function is known to exist. MDS algorithms provide a mathematical framework within which kriging and SGS can be applied and the original SPD matrix is approximately reproduced in the high dimensional space.

Estimation and simulation algorithms form the core of geostatistical reserve calculations. This paper summarized methodologies for IDW, kriging and SGS implementations that incorporate LVA. With these tools reserve estimation methodologies, such as Journel and Kyriakidis (2004), can be modified to incorporate LVA.

References

Babak O. and Deutsch C. V., 2008. Statistical approach to inverse distance interpolation. Stochastic Environmental Research and Risk Assessment. DOI 10.1007/s00477-008-0226-6.

Christakos G. 1984. On the problem of permissible covariance and variogram models. Water resources research 20(2):251-265.

Cressie, N., 1991, Statistics for spatial data: Wiley, New York, 928 p.

Curriero F 2005. On the use of non-Euclidean distance measures in geostatistics. Mathematical Geology 38(8):907-926.

Deutsch C.V. and Journel A., 1998. GSLIB - geostatistical software library and user's guide: New York, Oxford University Press, 369 p.

Deutsch C. V., 2002. Geostatistical Reservoir Modeling. New York, Oxford University Press, 376 p.

Dijkstra E.W., 1959. A Note on Two Problems in Connection With Graphs, Numerische Mathematik, 1(1):269-271.

Isaaks E. and Srivastava R., 1989. Introduction to Applied Geostatistics. New York, Oxford University Press, 561 p.

Isaaks, E., 1991. The application of Monte Carlo methods to the analysis of spatially correlated data. PhD Thesis, Stanford University, 226 p.

Journel A. and Kyriakidis P., 2004. Evaluation of Mineral Reserves: A Simulation Approach. Oxford University Press. 232 p.

Kennel M., 2004. KDTREE 2: Fortran 95 and C++ software to efficiently search for near neighbors in a multi-dimensional Euclidean space. eprint arXiv:physics/0408067.

Matheron G., 1973, The intrinsic random functions and their applications: Adv. Appl. Probab., 5:439–468.

Sampson P. and Guttorp P., 1992. Nonparametric estimation of nonstationary spatial covariance structure. J. Am. Statist. Assoc. 87:108–19.

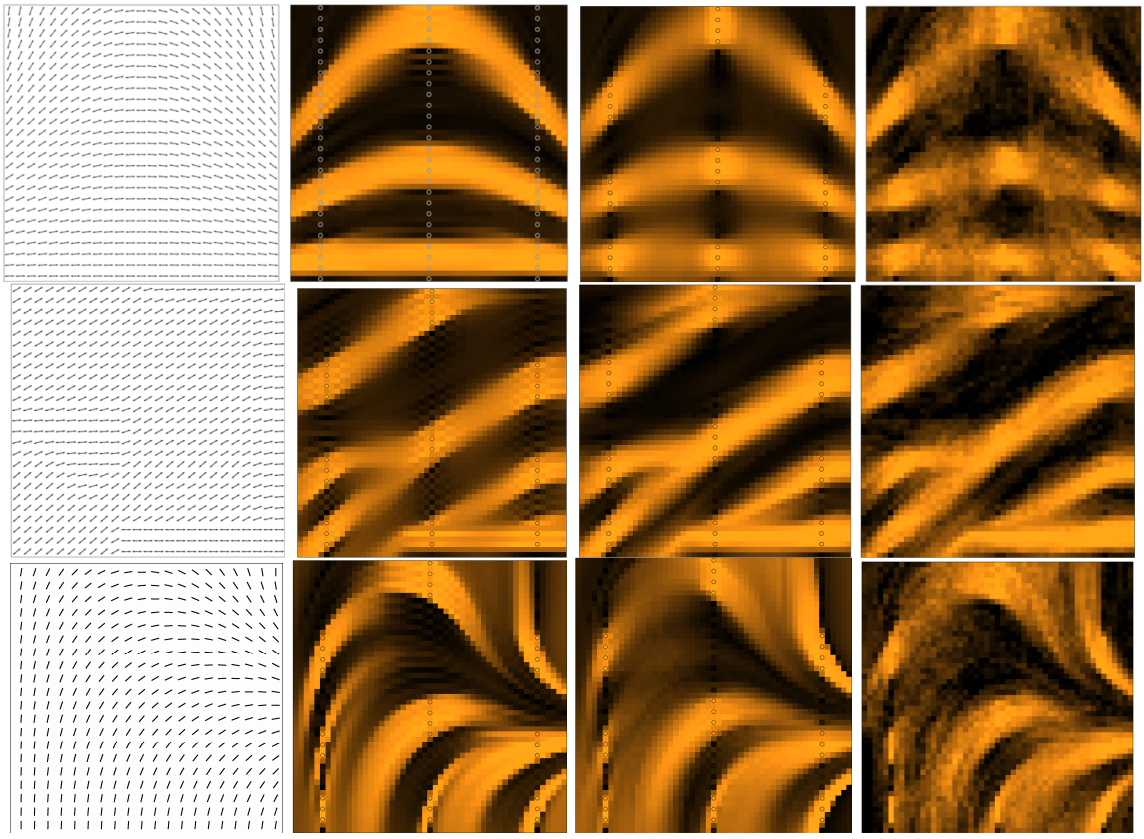

Figure 14: Examples of kriging with LVA. Left: LVA field direction, anisotropy ratio is constant 10:1. Middle Left: Estimates with IDW. Middle Right: Estimates with kriging with an exponential variogram with a range of 200 units. Right: SGS. Dimensions of all plots are 51x51 units. The same data strings with 78 total data were used. Scale ranges from black = 0 to orange/gray=6.